Au-Catalyst Assisted MOVPE Growth of CdTe Nanowires for Photovoltaic Applications

Virginia Di Carlo, Fabio Marzo, Massimo Di Giulio, Paola Prete and Nico Lovergine

Abstract Vertically-aligned CdTe nanowire (NWs) were grown for the first time by metalorganic vapor phase epitaxy, using diisopropyl-telluride and dimethyl-cadmium as precursors, and Au nanoparticles as metal catalysts. The NWs were grown between 485 and 515 °C on (111)B-GaAs substrates, the latter overgrown with a 2-μm thick CdTe epilayer. To favor the Au-catalyst assisted process against planar deposition of CdTe, an alternate precursors flow process was adopted during NW self-assembly. Field emission electron microscopy observations and X-ray energy dispersive analyses of CdTe NWs revealed the presence of Au-rich droplets at their tips, the contact-angle between Au-droplets and NWs being ∼130°. The NW height increases exponentially with the growth temperature, indicating that the Au-catalyzed process is kinetics-limited (activation energy: ∼57 kcal/mol), but no tapering is observed. Low temperature cathodoluminescence spectra recorded from single NWs evidenced a band-edge emission typical of zincblend CdTe, and a dominant (defects-related) emission band at 1.539 eV.

Keywords CdTe nanowires · Au-catalyzed growth · Metalorganic vapor phase epitaxy · Cathodoluminescence

1 Introduction

Quasi 1-dimensional nanostructures, so-called nanowires (NWs), based on III–V and II–VI compound semiconductors show novel and interesting physical properties, which make them particularly attractive for potential applications as functional

V. Di Carlo · F. Marzo · N. Lovergine (✉)
Dipartimento di Ingegneria dell'Innovazione, Università del Salento, Lecce, Italy
e-mail: nico.lovergine@unisalento.it

M. Di Giulio
Dipartimento di Fisica e Matematica "E. De Giorgi", Università del Salento, Lecce, Italy

P. Prete
Istituto per la Microelettronica e Microsistemi del CNR, Lecce, Italy

A. Leone et al. (eds.), *Sensors and Microsystems*, Lecture Notes in Electrical Engineering 457, https://doi.org/10.1007/978-3-319-66802-4_35

building blocks in nanoscale optical and optoelectronic devices [1]. Over the past decade, extensive studies on single semiconductor NWs and NW-based arrays have explored the device potentials of these nanomaterials as platforms for a new generation of high-efficiency and low-cost photovoltaic solar cells [2]. The incorporation of semiconductor NW structures into thin film solar cells offers the potential to overcome losses associated with minority carrier recombination, improve carrier mobility, and reduce optical reflection, allowing for increased photon collection efficiency [3]. Nanowire-based solar cells have developed rapidly, increasing their solar to electric power conversion efficiencies (PCE) from 5 to above 15% in the last 5 years [4]. Researches on next-generation photovoltaics aim to achieve PCE figures greater than 21%, approaching those (28–30%) expected theoretically [5].

CdTe is currently one of the most important semiconductors used for the fabrication of low-cost thin-films photovoltaic solar cells [6]. Indeed, its near-infrared band gap ($E_g \sim 1.5$ eV at 300 K [7]) matches the range of maximum solar irradiance spectrum, and its large bulk absorption coefficient ($>10^4$ cm^{-1} in the red, approaching 10^5 cm^{-1} in the blue [8]) makes it an excellent light harvester for solar energy applications. Compared with its thin film and bulk counterparts CdTe NWs are expected to be promising building blocks in the design of high-efficiency photovoltaic devices. Recent reports on the topic have focused on the fabrication of solar cells based on CdTe core-triple shell NWs, and demonstrated PCE figures $\sim$2.5% [9]. To further improve this value, a main challenge is the development of suitable synthesis techniques enabling the growth of CdTe NWs with high purity, and good crystalline and electronic properties, along with a suitable control of their diameter, height and density.

Currently, NWs of a broad range of semiconductors, such as Si, Ge [10, 11], III–V [12, 13] and II–VI [14, 15] are grown by either chemical vapor deposition (CVD), thermal evaporation, solvothermal synthesis, molecular-beam exitaxy (MBE) or metalorganic vapor phase epitaxy (MOVPE) utilizing the metal-catalyst assisted (so-called vapor-liquid-solid, VLS) mechanism [16, 17]. Through the years VLS growth has emerged as a straightforward technique for growing large quantities of inorganic single crystalline nanowires [18–20]. The technique stems from the ability of a metal (the catalyst) to form a low melting point alloy with one or more metal elements constituting the semiconductor crystal. For temperatures above the eutectic melting point, the catalyst behaves as solvent for the semiconductor metal element (s), the latter supplied from the gas phase (the Vapour), so that the amount of these elements inside the catalyst droplet eventually increases, leading to the formation of a supersaturated liquid droplet (the Liquid) and consequently, to the nucleation and growth of the semiconductor nanowire (the Solid). A most common metal-catalyst used for the VLS growth of semiconductor NWs is Au.

Few reports have been published to date on the VLS synthesis of tellurium-based semiconductor NWs; in particular, only very few have dealt with the Au-catalyzed self-assembly of CdTe NWs [21–23]. None of them has concerned the NW growth by the MOVPE technology.

In this study we describe a new method, i.e. the alternate precursors flow process, especially developed for the Au-catalyzed MOVPE growth of CdTe NWs, and

report in details on the conditions leading to NW self-assembly. After showing that the NWs do growth indeed by the VLS mechanism we report on the kinetics of the VLS process; we also present the morphological and optical properties of as-grown NWs. Finally, the results of low temperature cathodoluminescence (CL) measurements performed on single CdTe nanowires are presented and discussed.

2 MOVPE Growth of CdTe Nanowire by the Separate Precursors Flow Process

CdTe nanowires were grown on (111)B-oriented semi-insulating GaAs substrates using a home-built atmospheric pressure MOVPE reactor. More specifically, GaAs (111)B substrates were first degreased in isopropanol vapors, etched in $4H_2SO_4$:H_2O_2:$2H_2O$ solution to remove native surface oxides, rinsed in deionized water and finally blown-dried under N_2, as described in details in Ref. [17]. As-treated substrates were then annealed at 460 °C for 10 min under pure H_2 in order to remove any residual oxides possibly remained on the GaAs surface. Next, a ~2 μm thick (111)-oriented CdTe buffer layer was epitaxially grown at 350 °C for 30 min, under a total H_2 flow of 4.55 slm. Diisopropyl-telluride ($^iPr_2Te$) and dimethylcadmium (Me_2Cd) were used as Cd and Te precursors, each supplied at a flow rate of 55 μmol/min.

As-prepared substrates were then covered with Au NPs, following two different methods: thermal de-wetting of UHV-evaporated Au thin films (thickness between 1 and 2 nm) or direct deposition from a colloidal solution [17]. In both cases, the as-prepared samples were further annealed for 10 min at 445 °C, under H_2 flow, with the aim to (i) allow the Au NPs formation of proper size and density, or (ii) eliminate any possible organic contaminants arising from the colloidal solution.

After raising the sample temperature up to the final growth value, varied between 485 and 515 °C, Te and Cd precursors were provided separately, as shown in Fig. 1. This is a new approach we have developed in order to inhibit the CdTe planar growth, which is otherwise quite efficient at temperatures above the Au-$AuTe_2$ eutectic melting point (~7 μm/h at 447 °C), i.e. if both precursors are simultaneously admitted to the reactor chamber. Instead, in the alternate precursor flow process a molar flow rate of 25 μmol/min of $^iPr_2Te$ is first provided for Δt_{Te} = 1–10 min to the vapor phase, after which 50 μmol/min of Me_2Cd are flowed over the sample for Δt_{Cd} = 10 min, as illustrated in details in Fig. 1b. While the first Te-flow step ensures the formation of liquid Au–Te alloy droplets onto the surface of the CdTe buffer layer, the subsequent Cd-flow step allows for Cd atoms to enter the liquid Au–Te alloy droplets and, upon reaching supersaturation, finally leads to the growth of CdTe NWs. During the time interval between the Te and Cd flow-steps, pure H_2 is flowed through the reactor chamber to remove unreacted $^iPr_2Te$ molecules from the sample surface and out of the vapor phase. In doing this

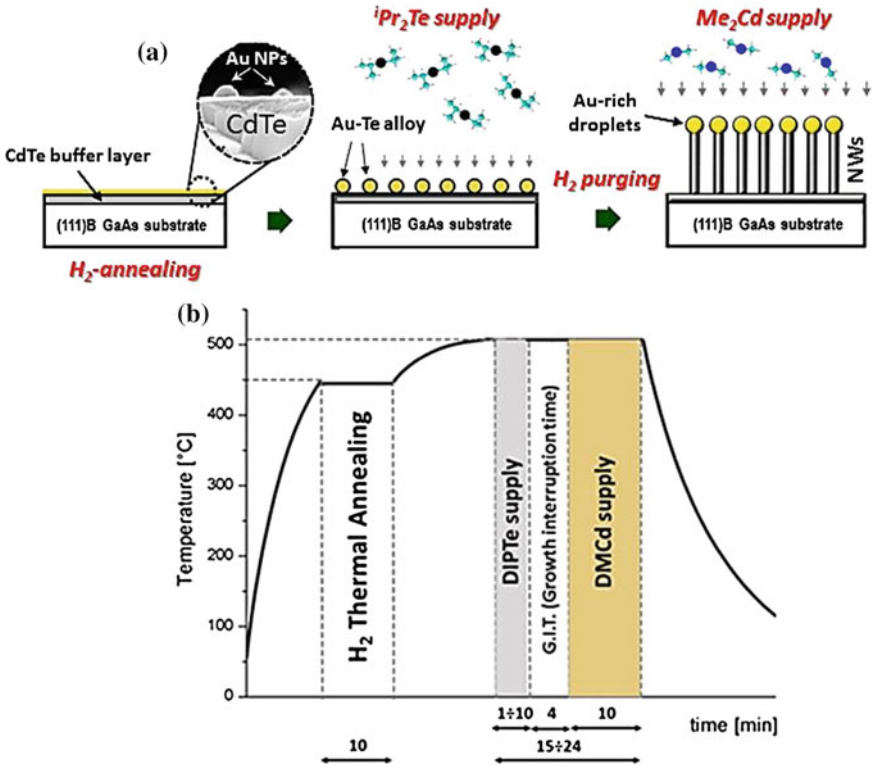

Fig. 1 **a** Schematic of the process steps adopted for the Au-catalyzed MOVPE growth of CdTe nanowires by the separate precursors flow process; **b** Process temperature profile and precursors supply sequence during the growth of CdTe nanowires

we ensure effective suppression of the planar growth rate during the NW self-assembly process. A detailed theoretical analysis of the actual growth mechanisms leading to the VLS growth of present CdTe NWs by the separate precursors flow method has been reported in Ref. [24]. Samples were cooled down to room temperature under pure H_2 flow.

3 Morphological, Structural and Optical Properties of As-Grown CdTe Nanowires

The separate precursors flow process allowed to successfully self-assemble CdTe NWs by MOVPE. Figures 2c shows a FE-SEM micrograph of an as-grown sample, confirming the occurrence of a high yield of straight vertically-standing NW structures, randomly distributed over the surface of the CdTe buffer layer. As the

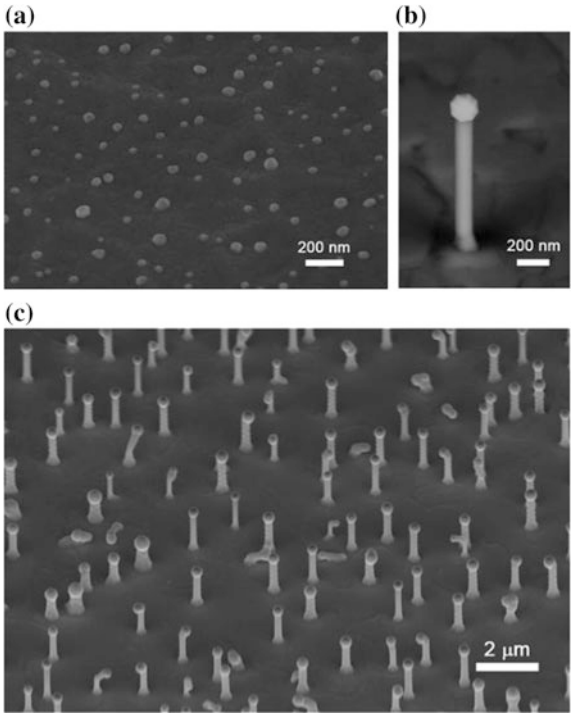

Fig. 2 FE-SEM micrographs (45° tilt-view) of (**a**) Au nanoparticles obtained by thermal de-wetting of 1-nm thick Au film after annealing at 445 °C for 10 min (120,000 × magnification); (**b**) a typical [111]-aligned CdTe nanowire grown at 507 °C (100,000 × magnification); and (**c**) a larger view (30,000 × magnification) of the sample surface in (**b**) showing a dense array of CdTe nanowires

CdTe epilayer is ⟨111⟩-oriented onto the GaAs substrate [24], this implies that the nanowire self-assemble homoepitaxially onto the buffer layer, with their major axis along the vertical ⟨111⟩ crystal direction, as commonly found for most Au-catalyzed III–V and II–VI nanowires [17, 24, 25].

In this work we used NPs obtained either (i) by self-assembling through the de-wetting of a thin evaporated Au film, or (ii) from colloidal solutions (NP average diameters ∼25 nm). Figure 2a shows the morphology of Au NPs as-obtained from de-wetting of a 1.1 nm thick Au film, upon thermal annealing under pure H_2 at 445 °C for 10 min. The annealing temperature was set below the Au–$AuTe_2$ eutectic melting point (447 °C) with the purpose to limit Au/substrate interactions. In this case, the surface density of Au NPs ranged around 2.4×10^9 cm^{-2}, but decreases to values in the 10^8 cm^{-2} range for samples obtained using the colloidal solution. However, the NW morphology remained independent on the way Au NPs were obtained.

All CdTe NWs grown in our experiments do show a quasi-spherical shaped nano-droplet at their upper tips, with average diameters in the range between 150–230 nm. Chemical information on the nano-droplet composition were obtained by spatially resolved energy dispersive X-ray spectroscopy (EDXS) measurements performed in the FE-SEM microscope. Figure 3 shows the results of EDXS analyses performed on single nano-droplets on top of CdTe nanowires, demonstrating

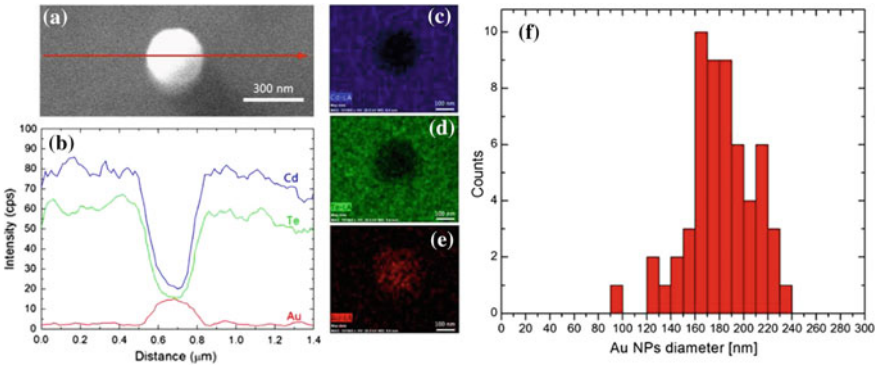

Fig. 3 SEM/EDXS analyses of a ~200 nm Au-rich NP on top of a [111]-aligned CdTe nanowire grown at 507 °C. **a** SEM micrograph (102,000 × magnification, plan-view) of the NP; **b** EDXS line scans [indicated by the *red arrow* in (**a**)] of Cd Lα (*blue*), Te Lα (*green*) and Au Lα (*red*) EDXS signals; EDXS maps of the same elements (same colors) are shown in (**c**–**e**); **f** Count histogram of the diameters of Au-rich NPs on top of CdTe nanowires grown at 507 °C (Color figure online)

that these droplets are made of an Au-rich alloy. In particular, Fig. 3b shows the Au, Cd, and Te Lα fluorescence signals obtained by scanning a 20 keV primary electron beam along the line drawn in red on the high magnification SEM micrograph of Fig. 3a. The Au EDXS signal intensity increases above the background level at the NP position; EDXS maps of the same elements performed by scanning the electron beam over a small area across the NP further confirmed that Au atoms are indeed concentrated inside the NP (Fig. 3e). This supports our conclusion that present CdTe NWs were grown by the Au-catalyzed (VLS) mechanism.

Figure 3f reports a typical count histogram of the Au-rich NP diameters at the top of CdTe nanowires, as measured from a series of plan-view FE-SEM micrographs.

With regard to the NW heights and diameters, present samples have shown a high degree of uniformity over broad enough surface areas, so that we have been able to investigate their size as function of growth temperature. The NWs showed diameters ranging from 60 to 350 nm and heights between 40 nm and 1.7 μm. Higher growth temperatures promoted their axial (i.e., in the $\langle 111 \rangle$-direction) elongation and a better size uniformity. In Fig. 4a the NW average heights are plotted on a semi-logarithmic scale as function of growth temperature (Arrhenius plot); the red curve is the Arrhenius function best-fitting the experimental data, corresponding to a process activation energy E_A = 56.8 kcal/mol. The NW diameter is also constant over their length, showing no indication of the tapering seen in other semiconductor systems [17, 26]. This implies a negligible growth of the material along the NW sidewalls. A count histograms of the NW diameters measured at the NW tip is reported in Fig. 4b. Some CdTe NWs show zigzagged sidewalls as also often observed for III-V NWs [27], which is ascribed to the presence of twin defects along the NW axis. As the energy of stacking fault

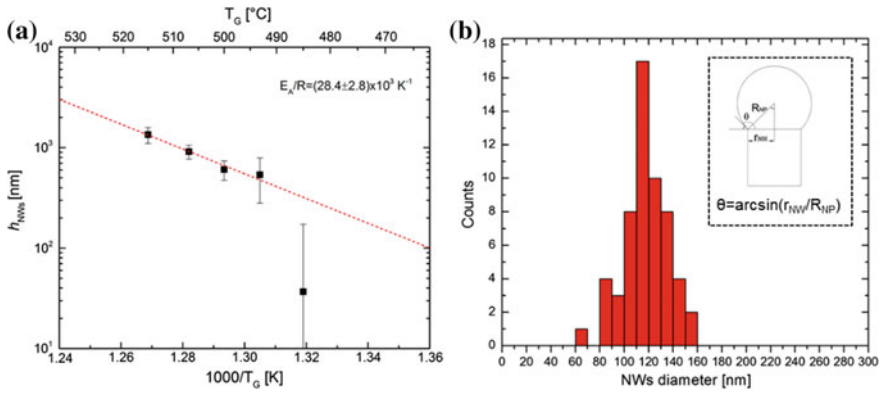

Fig. 4 **a** Arrhenius plot of the nanowire mean height (symbols) as a function of growth temperature ($\Delta t_{Te} = 1$ min). *Error bars* represent standard deviations. The *dashed* (*red*) *line* is the Arrhenius exponential function best-fitting the experimental data above 490 °C, and corresponding to an activation energy E_A = (56.8 ± 5.6) kcal/mol; **b** Count histogram of the diameters of CdTe nanowires grown at 507 °C; *Inset* in (**b**): geometrical definition of the nanowire radius (r_{NW}), the Au-NP radius (R_{NP}) and the Au-NP/nanowire contact angle (θ) (Color figure online)

(SF) formation in CdTe is fairly low (31–34 erg/cm^2), formation of SFs and twinned-crystal sections is thus expected during the VLS of CdTe NWs. Finally, NW growth below 485 °C resulted in the formation of nearly-hexagonal hillocks onto the CdTe buffer surface with Au-rich NPs still occurring at their tops.

We finally evaluated the average contact angle (θ) between the Au-rich NP and the underlying CdTe nanowire trunk by FE-SEM measurements of the Au NP (R_{NP}) and nanowire (r_{NW}) radius [24]. For all nanowires the estimated value of θ appears quite monodispersed around an average value of 130.5°, and independent on the actual nanowire growth temperatures. Interestingly, this result is in reasonable agreement with values reported in the literature for Au-catalyzed GaAs nanowires [28].

Low temperature CL spectra were recorded from single NWs after removing them from the original growth substrate; to this purpose, the nanowire samples were gently sonicated in isopropanol and the as-obtained solution poured onto Au-evaporated Si substrates. Figure 5a shows the CL spectrum collected at 7 K for one such single CdTe nanowire: the spectrum displays a well resolved band-edge emission at around 1.604 eV, as typical of zincblend CdTe (E_g = 1.6063 eV at 4.2 K, Ref. [29]). The NW shows also a broad and dominant band peaked at around 1.539 eV, possibly associated with a transition involving an acceptor level and likely due to Cd vacancies or Te interstitial defects. Interestingly, the CL emission appears uniform along the NW trunk (Fig. 5b). More details and in-depth analyses of the radiative properties of as-grown CdTe NWs are reported in our recent publication [24].

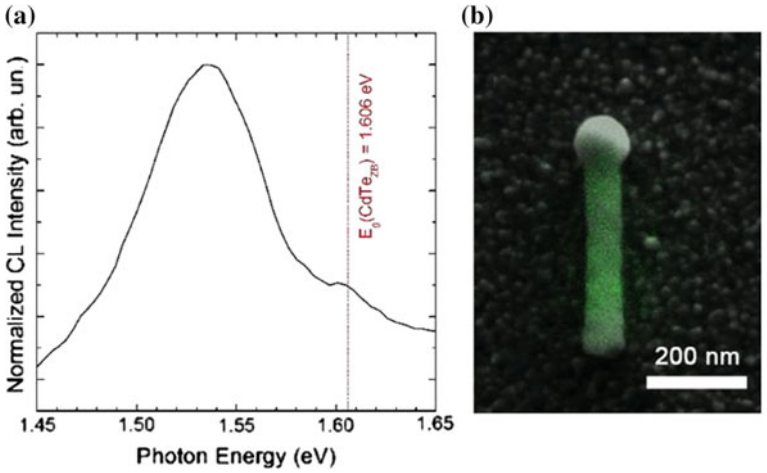

Fig. 5 **a** CL spectrum collected at 7K from a single CdTe nanowire after sonication and transfer onto an Au/Si substrate; **b** overlapping of a FE-SEM (*grey scale*) and a panchromatic-CL (*green color*) images recorded from the same CdTe nanowire

4 Conclusions

In summary, we demonstrated for the first time the growth of CdTe nanowires by MOVPE through the alternate precursors flow method, a new approach especially devised for the Au-catalyzed growth of CdTe nanowires above 485 °C. The method allows to suppress the conventional planar growth of CdTe in favor of the NW self-assembly by the VLS mechanism. An Au-rich droplet was found at the tip of each NW, confirming that CdTe nanostructures were indeed grown by the VLS process. FE-SEM observations allowed us to analyse the NW morphology and size as function of growth temperature. The NWs appear vertically-aligned along the substrate [111]-direction, the contact angle between the Au-rich NP and the NW being estimated $\sim$130°. The NW axial growth rate appears kinetically-activated and we estimated a process activation energy $\sim$57 kcal/mol. Analyses of the CL emission of single CdTe NWs has shown that as-grown nanostructures display a well resolved band-edge emission typical of zincblend CdTe, and a dominant (defect-related) broad band at around 1.539 eV.

Although additional work appears necessary with the purpose of further improving the growth process and the NW properties, present results open the path towards the manufacturing of high-efficiency CdTe/CdS nanowire-based solar cells by the MOVPE technology.

Acknowledgments The authors would like to acknowledge the financial support of the Ministry for Education, University and Research (MIUR) of Italy through the PON-R&C project INNOVASOL (project no. PON02-00323-3858246).

References

1. LaPierre, R.R., Robson, M., Azizur-Rahman, K.M., Kuyanov, P.: A review of III–V nanowire infrared photodetectors and sensors. J. Phys. D Appl. Phys. **50**, 123001 (2017)
2. Kempa, T.J., Day, R.W., Kim, S., Park, H., Lieber, C.M.: Semiconductor nanowires: a platform for exploring limits and concepts for nano-enabled solar cells. Energy Environ. Sci. **6**, 719–733 (2013)
3. Kapadia, R., Fan, Z., Javey, A.: Design constraints and guidelines for CdS/CdTe nanopillar based photovoltaics. Appl. Phys. Lett. **96**, 103116 (2010)
4. Otnes, G., Borgström, M.T.: Towards high efficiency nanowire solar cells. Nano Today **12**, 31–45 (2017)
5. Schockley, W., Qeisser, H.J.: Detailed balance limit of efficiency of p-n junction solar cells. J. Appl. Phys. **32**, 510–519 (1961)
6. Mathew, X., Thompson, G.W., Singh, V.P., McClure, J.C., Velumani, S., Mathews, N.R., Sebastian, P.J.: Development of CdTe thin films on flexible substrates—a review. Sol. Energy Mater. Sol. Cells **76**, 293–303 (2003)
7. Landolt-Bornstein: Numerical Data and Functional Relationships in Science and Technology, Springer, New York, New Series, Group III, 17a and 22a (1982)
8. Mitchell, K., Fahrenbruch, A.L., Bube, R.H.: Evaluation of the CdS/CdTe heterojunction solar cell. J. Appl. Phys. **48**, 829–830 (1977)
9. Williams, B.L., Taylor, A.A., Mendis, B.G., Phillips, L., Bowen, L., Major, J.D., Durose, K.: Core-shell ITO/ZnO/CdS/CdTe nanowire solar cells. Appl. Phys. Lett. **104**, 053907 (2014)
10. Kodambaka, S., Tersoff, J., Reuter, M.C., Ross, F.M.: Diameter-independent kinetics in the vapor-liquid-solid growth of Si nanowires. Phys. Rev. Lett. **96**, 096105 (2006)
11. Zakharov, N.D., Werner, P., Gerth, G., Schubert, L., Sokolov, L., Gösele, U.: Growth phenomena of Si and Si/Ge nanowires on Si (1 1 1) by molecular beam epitaxy. J. Cryst. Growth **290**, 6–10 (2006)
12. Ohlsson, B.J., Björk, M.T., Magnusson, M.H., Deppert, K., Samuelson, L., Wallenberg, L.R.: Size-, shape-, and position-controlled GaAs nano-whiskers. Appl. Phys. Lett. **79**, 3335–3337 (2001)
13. Duan, X., Huang, Y., Cui, Y., Wang, J., Lieber, C.M.: Indium phosphide nanowires as building blocks for nanoscale electronic and optoelectronic devices. Nature **409**, 66–69 (2001)
14. Huo, H.B., Dai, L., Liu, C., You, L.P., Yang, W.Q., Ma, R.M., Ran, G.Z., Qin, G.G.: Electrical properties of Cu-doped p-ZnTe Nanowires. Nanotechnology **17**, 5912–5915 (2006)
15. Chan, S.K., Cai, Y., Wang, N., Sou, I.K.: Growth temperature dependence of MBE-grown ZnSe Nanowires. J. Cryst. Growth **301–302**, 866–870 (2007)
16. Wagner, R.S., Ellis, W.C.: Vapor-liquid-solid mechanism of single crystal growth. Appl. Phys. Lett. **4**, 89–90 (1964)
17. Paiano, P., Prete, P., Lovergine, N., Mancini, A.M.: Size and shape control of GaAs nanowires grown by metalorganic vapor phase epitaxy using tertiarybutylarsine. J. Appl. Phys. **100**, 094305 (2006)
18. Fan, H.J., Werner, P., Zacharias, M.: Semiconductor nanowires: from self-organization to patterned growth. Small **2**, 700–717 (2006)
19. Dick, K.A.: A review of nanowire growth promoted by alloys and non-alloying elements with emphasis on Au-assisted III–V nanowires. Progr. Cryst. Growth Character. Mater. **54**, 138–173 (2008)
20. Chen, C.C., Yeh, C.C., Chen, C.H., Yu, M.Y., Liu, H.L., Wu, J.J., Chen, K.H., Chen, L.C., Peng, J.Y., Chen, Y.F.: Catalytic growth and characterization of gallium nitride nanowires. J. Am. Chem. Soc. **123**, 2791–2798 (2001)
21. Wojtowicz, T., Janik, E., Zaleszczyk, W., Sadowski, J., Karczewski, G., Dluzewski, P., Kret, S., Szuszkiewicz, W., Dynowska, E., Domagala, J., Aleszkiewicz, M., Baczewski, L.T., Petroutchik, A., Presz, A., Pacuski, W., Golnik, A., Kossacki, P., Morhange, J.F., Kirmse, H.,

Neumann, W., Caliebe, W.: MBE growth and properties of ZnTe- and CdTe-based nanowires. J. Korean Phys. Soc. **53**, 3055–3063 (2008)
22. Ye, Y., Dai, L., Sun, T., You, L.P., Zhu, R., Gao, J.Y., Peng, R.M., Yu, D.P., Qin, G.G.: High-quality CdTe nanowires: synthesis, characterization, and application in photoresponse devices. J. Appl. Phys. **108**, 044301 (2010)
23. Williams, B.L., Halliday, D.P., Mendis, B.G., Durose, K.: Microstructure and point defects in CdTe nanowires for photovoltaic applications. Nanotechnology **24**, 135703 (2013)
24. Di Carlo, V., Prete, P., Dubrovskii, V.G., Berdnikov, Y., Lovergine, N.: CdTe nanowires by Au-catalyzed metalorganic vapor phase epitaxy. Nano Lett. **17**, 4075–4082 (2017)
25. Seifert, W., Borgström, M., Deppert, K., Dick, K.A., Johansson, J., Larsson, M.W., Mårtensson, T., Sköld, N., Svensson, C.P.T., Wacaser, B.A., Wallenber, L.R., Samuelson, L.: Growth of one-dimensional nanostructures in MOVPE. J. Cryst. Growth **272**, 211–220 (2004)
26. Ihn, S.-G., Song, J.-I., Kim, T.-W., Leem, D.-S., Lee, T., Lee, S.-G., Koh, E.K., Song, K.: Morphology- and orientation-controlled gallium arsenide nanowires on silicon substrates. Nano Lett. **7**, 39–44 (2007)
27. Wolf, D., Lichte, H., Pozzi, G., Prete, P., Lovergine, N.: Electron holographic tomography for mapping the three-dimensional distribution of electrostatic potential in III-V semiconductor nanowires. Appl. Phys. Lett. **98**, 264103 (2011)
28. Sakong, S., Du, Y.A., Kratzer, P.: Atomistic modeling of the Au droplet-GaAs interface for size-selective nanowire growth. Phys. Rev. B **88**, 155309 (2013)
29. Landolt-Börnstein. In: Madelung, O., Van der Osten, W., Rössler, U. (eds.) Semiconductors: Intrinsic Properties of Group IV Elements and III–V, II–VI and I–VII Compounds, III-22. Springer, Berlin (1987)